IEEE Access
Multidisciplinary | Rapid Review | Open Access Journal

Received 26 September 2022, accepted 7 December 2022, date of publication 12 December 2022,
date of current version 20 December 2022.

Digital Object Identifier 10.1109/ACCESS.2022.3228570

RESEARCH ARTICLE

An Artificial Neural Network-Based Handover Scheme for Hybrid LiFi Networks

GUANGHUI MA, (Member, IEEE), RAJENDRAN PARTHIBAN, (Senior Member, IEEE), AND NEMAI KARMAKAR, (Senior Member, IEEE)
Department of Electrical and Computer Systems Engineering, Monash University, Clayton, VIC 3800, Australia
Corresponding author: Guanghui Ma (guanghui.ma@monash.edu)

ABSTRACT Combining the ultra-high user throughput of the light fidelity (LiFi) and the ubiquitous coverage of wireless fidelity (WiFi), the hybrid LiFi and WiFi network (HLWNet) demonstrates unparalleled advantages in indoor wireless data transmission. Due to the line-of-sight propagation nature of the optical signal, the handover decision-making problem in HLWNets, however, becomes more critical and challenging than that in previous heterogeneous networks. In this paper, the handover decision-making problem in the HLWNet is regarded as a binary classification problem, and an artificial neural network (ANN)-based handover scheme is proposed. The complete handover scheme consists of two sets of ANNs that use the information about channel quality, user movement, and device orientation as input features to make handover decisions. After being trained with the labeled datasets that are generated with a novel approach, the ANN-based handover scheme is able to achieve over 95% handover accuracy. The proposed scheme is then compared with benchmarks under an indoor simulation scenario. The simulation results show that the proposed approach can significantly increase user throughput by $20.5-46.7\%$ and reduce handover rate by around $59.5-78.2\%$ as compared with the benchmarks; in the meanwhile, it maintains a great robustness performance against user mobility and channel variation.

INDEX TERMS Handover, light fidelity (LiFi), machine learning (ML), sixth-generation wireless network (6G), visible light communication (VLC), wireless fidelity (WiFi).

I. INTRODUCTION

Although the fifth-generation (5G) wireless communication network has already been standardized and commercialized worldwide since 2020, its current performance will no longer be adequate in the foreseeable future due to the booming growth of new industries such as the Internet of things (IoT) and mobile virtual reality (VR) technologies [1], [2]. Compared with the 5G, the next-generation wireless network or the sixth-generation (6G) wireless network is expected to be human-centric, and in the meanwhile provides higher data rates, stronger privacy, and higher energy/cost efficiency [3].

The hybrid light fidelity (LiFi) and wireless fidelity (WiFi) network (HLWNet) has continuously attracted research interest and been regarded as a potential component of the 6G network [4]. Especially in indoor scenarios, the HLWNet demonstrates unparalleled advantages over conventional radio frequency (RF) heterogeneous networks (HetNets) [5], [6]. On the one hand, the light emitting diode (LED) based LiFi network is able to provide ultra-high data transmission with great power efficiency, low interference, and high physical layer security. WiFi, on the other hand, works as a substitute for LiFi when the optical signal is unavailable to enhance signal continuity and user mobility [7]. However, due to the ultra-dense deployment of LiFi access points (APs) and the susceptible LoS propagation nature of the optical light, the handover decision-making between LiFi and WiFi becomes more critical than that in conventional heterogeneous networks [8].

According to our previous study in [9], a typical handover scheme consists of three modules, including the information gathering module (IGM), the decision-making

The associate editor coordinating the review of this manuscript and approving it for publication was Seifedine Kadry.

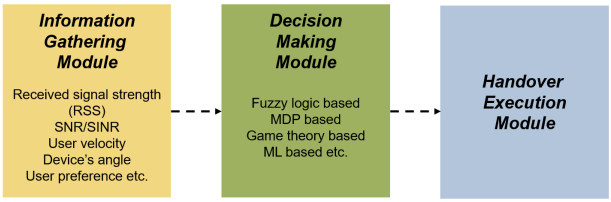

FIGURE 1. A three-module handover scheme.

module (DMM), and the handover execution module (HEM), as depicted in Fig. 1. The IGM collects all the information required for the handover decision-making and periodically passes the information to the DMM, where the handover algorithm locates. The DMM then decides the most suitable access network and whether to perform the handover to it. The handover is triggered once the HEM receives the handover request from the DMM.

The handover algorithm that gives the rules for decision-making plays the most important role in the handover scheme design. Mathematically, the handover algorithm can be regarded as a multiple-input single-output function, where the inputs are the values of all metrics used for the handover decision-making and the output, equivalent to either "0" or "1", indicates the decision result. Any mathematical tool that approximates this type of functions can be used to design a handover algorithm. Many math models, including fuzzy logic (FL) [10], [11], Markov decision process (MDP) [12], [13] [14], and game theory (GT) [15], [16], have been applied for the handover algorithm design in heterogeneous visible light communication (VLC) and RF networks. In our previous work, we regard the handover problem in the HLWNet as a pattern recognition problem, more specifically a binary classification problem, for the first time [17]. The logistic regression (LR) and the support vector machine (SVM) have been applied to design the handover algorithms. Although the simulation results show that the LR- and the SVM-based handover methods outperform the previous handover schemes, their handover accuracy is hard to be improved further due to the inherent disadvantage of solving the non-linear boundary classification problem of these two methods.

To further increase the handover accuracy and improve the other handover metrics, we investigate the artificial neural network (ANN) in the handover decision-making in the HLWNet, due to its capability of solving non-linear problems without explicit models [18], [19] [20]. There have been a handful of attempts to apply ANN to the handover management problems in heterogeneous VLC-RF networks. To increase the user throughput of mobile users, [8] adopts an ANN to adjust the selection preference between LiFi and WiFi access networks. This work has shown the superiority of the ANN in handover algorithm design; however, there are still a number of research gaps in this study. First, the complex indoor user behavior such as device orientation is neglected in the decision-making. Furthermore, instead of deciding whether to execute the handover with given inputs

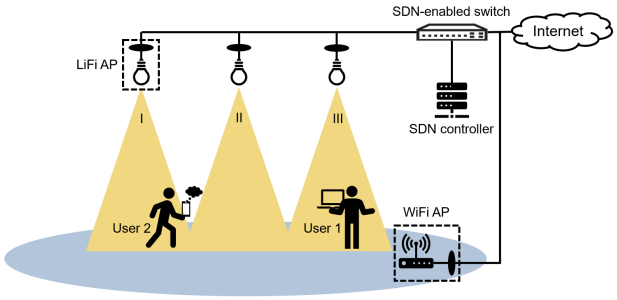

FIGURE 2. A software-defined networking (SDN) based HLWNet structure [21].

straightaway, the ANN-based algorithms in [8] only provides the network preference score. Extra procedures are needed to make a complete handover decision.

Aiming at the issues mentioned above, we propose a novel ANN-based handover scheme, in which we regard the handover problem in HLWNets as a binary classification problem as we did in [17]. The proposed scheme consists of two ANNs: one is for the handover decision-making from LiFi to WiFi and the other one is for the handover decision-making from WiFi to LiFi. Compared with the ANN-based handover scheme in [8], our methods have two main advantages. Firstly, since multiple attributes such as channel quality, light-path blockage, user mobility, and device orientation have been considered as features for the ANNs, our method can make more timely, precise, and reliable decisions. Additionally, our proposed method avoids redundant handover decision procedures. Since the handover is regarded as a binary classification problem, the proposed scheme is able to make the handover decision with a set of given inputs straightforward.

The simulation results show that the proposed scheme achieves above 95% handover accuracy, near-optimal user throughput, and a significant handover rate reduction as compared to the benchmarks. In addition, the proposed method shows superior robustness performance against different working scenarios.

The remainder of the paper is organized as follows. The HLWNet model is introduced in Section II. Section III demonstrates the novel ANN-based handover scheme. Section IV presents the simulation results and related discussion. Finally, the conclusions are drawn in Section V.

II. SYSTEM MODELS

An HLWNet system consisting of multiple LiFi APs and a single WiFi AP is used for this study. To avoid interference to the LiFi downlink transmission, we adopt a bidirectional LiFi network scheme that uses visible light for the downlink and IR for the uplink communication [22]. Each LiFi cell consists of a pair of LED and infrared (IR) photodetector (PD) as the transceiver, which is assumed to be facing vertically downwards. In addition, all LiFi and WiFi APs are connected to software-defined networking (SDN)-enabled switch via SDN agents, and the data packets from the Internet will

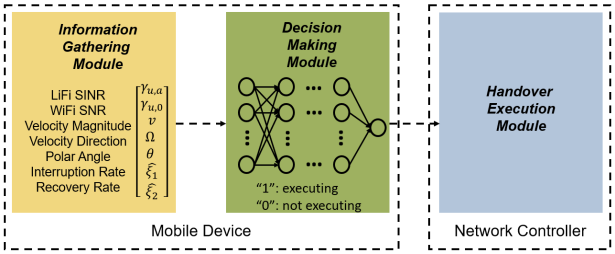

FIGURE 3. The working procedure of the proposed ANN-based handover scheme.

be routed to each AP under the supervision of the network controller, as shown in Fig. 2 [7], [21]. In each LiFi cell, time division multiple access (TDMA) is employed as the multiple access scheme, whereas carrier-sense multiple access with collision avoidance (CSMA/CA) is applied as the medium access control (MAC) for the WiFi network [23].

The system models used for this study, including the LiFi channel model, WiFi channel model, the achievable data rate of both LiFi and WiFi, the modified orientation-based random waypoint (ORWP) model, and the light-path blockage, are the same as our previous work in [9]. The variable notations are also the same as those in [9]. Please refer to Section II of [9] for details.

III. ANN-BASED HANDOVER SCHEME

In this section, we propose a novel ANN-based handover scheme that regards the handover decision as a binary classification problem. The working procedure of the proposed handover scheme is quite straightforward, as shown in Fig. 3. The information about the current/target channel quality, light-path blockage, user mobility, and device orientation is gathered periodically by the IGM which locates in the user equipment (UE). Since only the vertical handover (VHO) is considered in our scheme, the IGM just needs to monitor the channel quality of the LiFi AP with the highest signal-to-interference-plus-noise ratio (SINR) and the WiFi AP [9]. The SINR/SNR information can be monitored in the mobile node [8], [24]. The user velocity and angular information can be measured by the inertial measurement unit (IMU) in smart devices [6], [25]. Furthermore, the average light-path available/unavailable period needs to be recorded and updated to calculate the estimated interruption and recovery rates, $\hat{\xi}_1$ and $\hat{\xi}_2$ [10]. The measured information is then wrapped up as an input vector for the pre-trained neural network. After transforming the inputs through a series of hidden layers which are made up of a set of neurons, the neural network finally outputs the handover decision. In our scheme, the output "1" means executing the handover immediately, whereas the output "0" means not executing the handover. Since the complete handover scheme consists of two parts, i.e. the handover from WiFi to LiFi and the handover from LiFi to WiFi, we need to train two sets of neural networks. In the following section, we will describe the ANN architecture, the dataset generation, the ANN training, and the ANN testing.

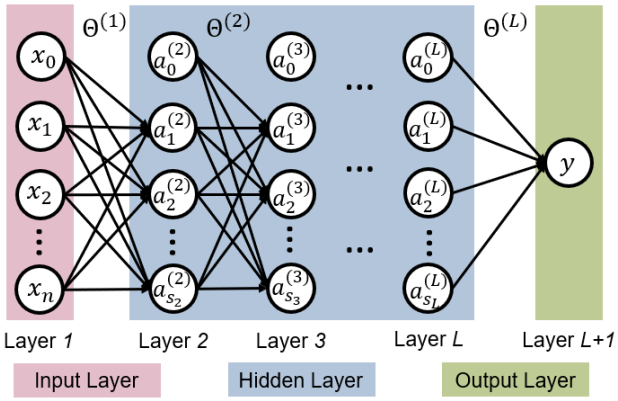

FIGURE 4. The architecture of a fully-connected L-layer ANN with 1 input layer, $L-1$ hidden layers, and 1 output layer.

A. ANN ARCHITECTURE

As mentioned in Section I, the handover algorithm can be regarded as a nonlinear function $f(\mathbf{x})$ with a single output either equal to "1" or "0", where $\mathbf{x} \in \mathbb{R}^n$ is the input vector that contains n features. Therefore, designing the handover algorithm is equivalent to finding the optimal approximator or hypothesis $h_\Theta(\mathbf{x}; \Theta)$ of the function $f(\mathbf{x})$. Neural network or ANN, modeled as collections of neurons, shows great potential to solve this problem since the neural network with at least one hidden layer, and proper activation functions can approximate any continuous function [26]. Combining the ANN with a maximum likelihood estimation (MLE) threshold, we can find an approximator function with an output equals "1" or "0". A fully-connected L-layer (not including input layer) ANN architecture, in which neurons between two adjacent layers are fully pairwise connected, is applied in this article, as shown in Fig. 4. As for each neuron, the sum of weighted outputs of the previous layer and a bias is fed in an activation function in it. The activation function is used to introduce non-linearity to the neuron. The computation process from the input layer to the output layer is called forward propagation, which is given by:

$$\begin{aligned} \mathbf{a}^{(1)} &= g(\Theta^{(1)} \begin{bmatrix} x_0 \\ \mathbf{x} \end{bmatrix}), \\ \mathbf{a}^{(j+1)} &= g(\Theta^{(j)} \begin{bmatrix} a_0^{(j)} \\ \mathbf{a}^{(j)} \end{bmatrix}), \\ h_\Theta(\mathbf{x}; \Theta) &= g(\Theta^{(L)} \begin{bmatrix} a_0^{(L)} \\ \mathbf{a}^{(L)} \end{bmatrix}), \end{aligned} \tag{1}$$

where L denotes the depth of the ANN; s_l is the number of neurons (not counting bias units) in layer l; $a_i^{(j)}$ is the activation of neuron i ($i \neq 0$) in layer j; x_0 and $a_0^{(j)}$ are the biases of the input vector and layer j respectively; $\Theta^{(j)} \in \mathbb{R}^{s_{(j+1)} \times (s_j+1)}$ is the matrix of weights controlling function mapping from layer j to layer $j+1$; $g(\cdot)$ denotes the sigmoid activation function with the expression as:

$$g(\mathbf{x}) = \{\frac{1}{1+e^{-\mathbf{x}}} \in (0,1)^n \mid \mathbf{x} \in \mathbb{R}^n\} \tag{2}$$

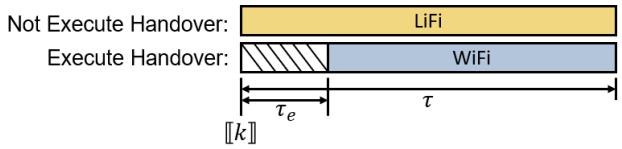

FIGURE 5. The UE is currently connected to the LiFi network and the shadow area is the handover execution period.

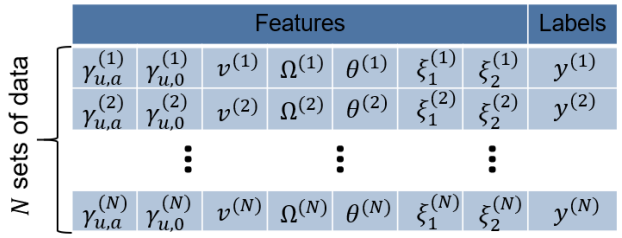

FIGURE 6. The architecture of the dataset with *N* sets of data.

Since the output of the hypothesis $h_\Theta(\mathbf{x};\Theta)$ indicates the estimated probability that $y = 1$ on input $\mathbf{x}$, a maximum likelihood estimator is needed in the output layer to achieve the "1/0" classification;

$$y = \begin{cases} 0, & h_\Theta(\mathbf{x};\Theta) < 0.5 \\ 1, & h_\Theta(\mathbf{x};\Theta) \geq 0.5. \end{cases} \tag{3}$$

Hence, for a neural network with well-trained parameters Θ, given an input vector $\mathbf{x}$, the DMM will send the handover request to the HEM if the output of the ANN, $y = 1$; otherwise, the UE will stay in the current network.

B. DATASET GENERATION

Adequate numbers of data with labeled ground truth are essential for supervised learning tasks; however, all previous works of the ANN-based handover algorithm, to the best of our knowledge, lack details on labeled data generation [8], [27] [28]. Unlike the other classification problem, such as object detection, it is not obvious to decide the target value with a set of given inputs; in other words, it is not clear whether the handover execution is worthwhile, though the information about the channel quality, user mobility, and the interruption/recovery rates is known. To build up the labeled datasets, we propose a novel approach that consists of the following steps:

1) First, we generate the tuple sequences of the dynamic information (including position, velocity, and polar angle) by the modified ORWP model in Section II-E of [9].
2) The SINR/SNR values of both LiFi and WiFi channels for each user at each moment are then calculated from the position, velocity direction, and polar angle information under the simulation scenarios described in Section II-A and B of [9].
3) The light-path blockage is introduced by the ON-OFF model with given interruption and recovery rates ξ_1 and ξ_2. For simplicity, the SINR of the LiFi channel is assumed to be 0 when the optical channel is blocked.

After implementing steps 1) to 3), we obtained the dataset for M users over the T_{SIM} simulation time:

$$\mathcal{D} \in \mathbb{R}^{K\times 7\times M},$$

where $K = T_{SIM}/\Delta t$ is the discrete time length.

1) Randomly choosing a time point k, the data required for the handover decision of UE m at this moment is denoted as:

$$\begin{aligned}(\mathbf{x}_k^{(m)})^T &= \mathcal{D}(k,:,m) \\ &= \left[\gamma_{u,a}\ \gamma_{u,0}\ v\ \Omega\ \theta\ \xi_1\ \xi_2\right]_k^{(m)},\end{aligned} \tag{4}$$

where $\mathbf{x}_k^{(m)}$ is the input vector for the neural network. As illustrated in Fig. 5, if the UE is connected to a LiFi AP and the average data rate of switching to the WiFi network in the following short period τ is greater than the rate of staying in the LiFi network, i.e.,

$$\int_{k+\tau_e}^{k+\tau} r_{u,0}\,\mathrm{d}t > \int_k^{k+\tau} r_{u,a}\,\mathrm{d}t, \tag{5}$$

where τ_e is the execution time, then we label $y = 1$, otherwise $y = 0$.

2) Feature scaling is needed to ensure that all features have the same scale. We end up with 10000 sets of data structured as shown in Fig. 6. With the same method, we have also created 10000 sets of data for the handover decision from WiFi to LiFi.

Both datasets are partitioned into three segments, in which the training (70%) and validation (15%) sets are for adjusting the hyperparameters and tuning the model; and the test (15%) set is used to assess the network performance.

C. TRAINING AND TESTING

After setting up the ANN architecture, we obtain a hypothesis $h(\mathbf{x};\Theta)$. Then, we need to work on the model training to adjust the hyperparameters Θ and to achieve the optimal performance. The data loss which measures the compatibility between a prediction and the ground truth is adopted to evaluate the hypothesis performance. In our work, the data loss is calculated by Eq. 6, as shown at the bottom of the next page, where N_{train} is the size of the training set. Therefore, training the ANN is transformed into an optimization problem,

$$\Theta^* = \arg\min_\Theta J(\Theta), \tag{7}$$

which is solved by the gradient descent algorithm in our work [29]. During the training process, the ANN model should also be tuned based on the cross validation [30]. Finally, the performance of the hypothesis is evaluated on the test set by checking the average loss plots, and the confusion matrices [31].

IV. SIMULATION RESULTS

A. SIMULATION PARAMETERS

An indoor office with dimensions of $18 \times 18 \times 3\text{m}^3$ is implemented as the default simulation scenario, which is equipped

TABLE 1. LiFi simulation parameters.

Parameter	Value
Room size, $a \times b$	$18 \times 18\text{m}^2$
Height from desk to ceiling, h	2.5m
Number of APs, N_A	36
Semi angle of half power, $\phi_{1/2}$	60°
Transmitted optical power of LiFi AP α, $P_{t,\alpha}$	9W
Physical size of a PD, A_{pd}	1cm^2
Field of view, Ψ_{max}	90°
Optical gain, $g_f(\psi)$	1
Refractive index of concentrator, n_i	1.5
Wall reflectivity, ρ_w	0.8
Optical to electric power conversion coefficient, ι	3
Detector responsivity, R_{pd}	0.53A/W
Noise PSD of LiFi channel, N_{LiFi}	$10^{-21}\text{A}^2/\text{Hz}$
Bandwidth of LiFi channel, B_{LiFi}	40MHz

TABLE 2. WiFi simulation parameters.

Parameter	Value
Carrier frequency, f_c	2.4GHz
Transmitted power of WiFi AP, $P_{t,0}$	20dBm
Breakpoint distance, d_{BP}	10m
Shadowing fading std. dev for LoS, σ_{SF}	3dB
Shadowing fading std. dev for NLoS, σ_{SF}	5dB
The arrival/departure angle of LoS component, ϕ_0	45°
Ricean K-factor for LoS, K	2
Ricean K-factor for NLoS, K	0
Noise PSD of WiFi channel, N_{WiFi}	-174dBm/Hz
Bandwidth of WiFi channel, B_{WiFi}	20MHz

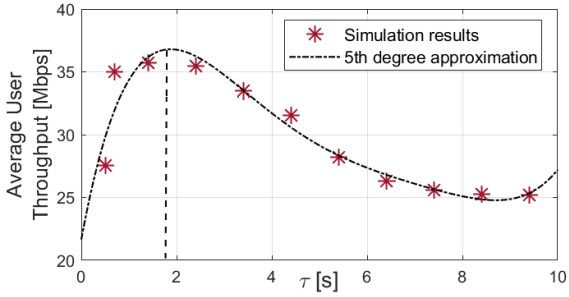

(a) The performance of the ANN-based handover scheme with only handovers from LiFi to WiFi.

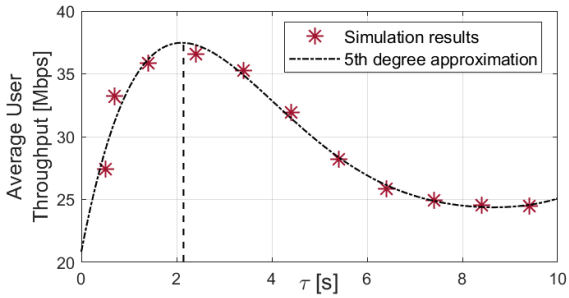

(b) The performance of the ANN-based handover scheme with only handovers from WiFi to LiFi.

FIGURE 7. The plots of average user throughput against different τ values.

with a 2.4GHz WiFi AP and 36 LED-based LiFi APs in a lattice topology. In addition, the kernelized LR(K-LR)-based, the kernelized SVM(K-SVM)-based, and the ANN-based handover algorithm (referred to as ANN*) [1] in [8] with the same simulation parameters, are adopted as benchmarks of the proposed ANN-based handover scheme (referred to as *proposed* ANN). The handover overhead is approximated as a normal distribution with an expected value of 400ms [10]. Additionally, 300 users, whose velocity magnitude and direction are uniformly distributed from $0-3$m/s and $0-2\pi$, are evaluated and each of them has a simulation time of 300s. Other simulation parameters are summarised in Tables 1 and 2.

B. ANN SPECIFICATIONS

As described in Section III-B, the datasets are labeled by checking whether the handover execution brings more benefits than keeping connected to the current AP in the following "τ" period. If the handover is worthwhile, the data vector is labeled with "1"; otherwise, it is denoted with "0".

[1]Because the authors of [8] do not provide their dataset or explain how they generate their dataset, we train their ANN model with our datasets here.

Therefore, the first task is to determine the optimal τ value that gives the best overall performance.

We first check the optimal τ of the dataset to train the ANN that makes the handover decision from LiFi to WiFi. We start by defaulting the depth of the ANN to 2, i.e. there is one hidden layer, which by default has 7 neurons and one bias. Suppose that the UE is currently connected to the LiFi network, different values of τ are chosen to label the 10000 sets of data, which are then used to train the neural network. After that, the trained hypothesis is used to simulate the average user throughput of the 100 users over 300s. As shown in Fig. 7a, we check the average user throughput against different τ values and then use 5th-degree polynomials to approximate the relation between them. It is found that the average user throughput of the proposed ANN-based handover scheme increases sharply and reaches its maximum when τ is around 1.9s. Then, the throughput decreases rapidly as the value of τ increases and eventually converges to around 25Mbps. This is because the measured inputs are only useful for the "near future" predictions but do not work for the long-term ones. In addition, the bell-shaped curve in Fig. 7a also indicates that it is feasible to employ a neural network to design a handover algorithm because if it did not work, the

$$J(\Theta) = -\frac{1}{N_{train}}[\sum_{i=1}^{N_{train}} y^{(i)} log(h_\Theta(\mathbf{x}^{(i)};\Theta)) + (1-y^{(i)}) log(1-h_\Theta(\mathbf{x}^{(i)};\Theta))] \quad (6)$$

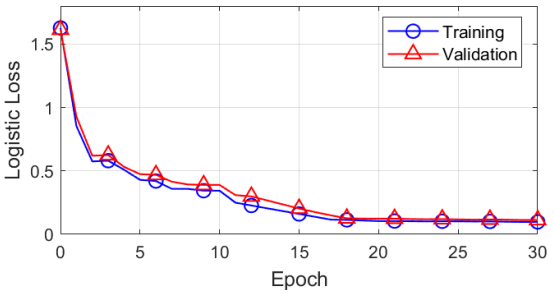

(a) The losses versus epoch index plot of the handover ANN from LiFi to WiFi.

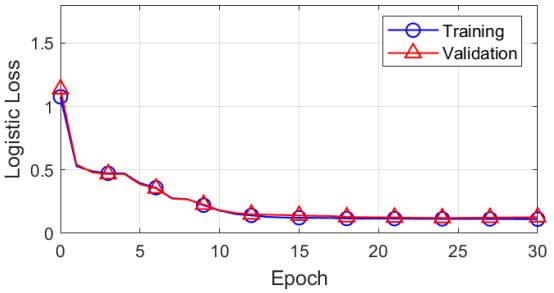

(b) The losses versus epoch index plot of the handover ANN from WiFi to LiFi.

FIGURE 8. Training and validation losses of the ANN versus the epoch index.

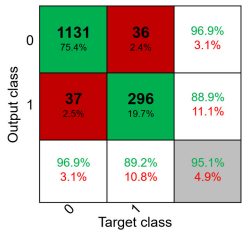

(a) The performance of the ANN that makes handover decisions from LiFi to WiFi.

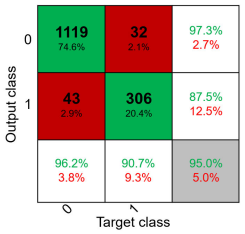

(b) The performance of the ANN that makes handover decisions from WiFi to LiFi.

FIGURE 9. Confusion matrices.

curve should be a horizontal line. Using the same approach, the optimal τ for the dataset to train the ANN that makes the handover decision from WiFi to LiFi is found located around 2.1s, as shown in Fig. 7b. Hence, the two optimal values, $\tau = 1.9$s and $\tau = 2.1$s, are applied to label two datasets to train the decision-making ANNs.

After obtaining the labeled datasets, we begin to train the ANNs for handover decision-making. We first train the ANN that makes handover decisions from LiFi to WiFi. The training and validation losses against the epoch index are shown in Fig. 8a. It shows that the training and validation losses decrease rapidly and converge to around the same amount as the epoch index increases. This indicates that our network is effective and that there is no overfitting.

The performance of the trained ANN is then checked with the test set and the results are presented in the confusion

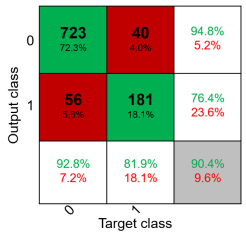

(a) K-LR handover scheme.

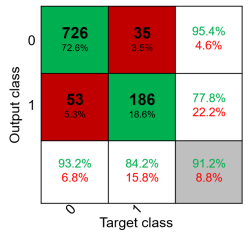

(b) K-SVM handover scheme.

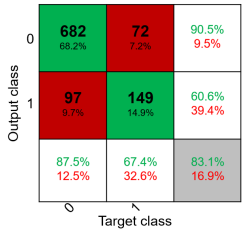

(c) ANN* handover scheme.

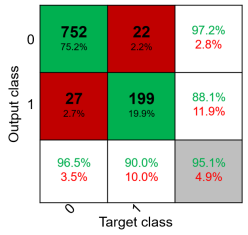

(d) The proposed ANN handover scheme.

FIGURE 10. The comparison of handover accuracy.

matrix in Fig. 9a. It is found that the proposed ANN model performs quite well and it can achieve a 95.1% accuracy with

$$F_1 \text{ score} = \frac{2(precision \times recall)}{precision + recall} = 0.89, \tag{8}$$

where $precision = 88.9\%$ and $recall = 89.2\%$. We have tried to improve the accuracy by increasing the number of hidden layers and neurons, but with limited improvement. Therefore, we believe that one hidden layer with 7 neurons and one bias is sufficient for this problem. With the same approach, we trained the other ANN that makes handover decisions from WiFi to LiFi with the second dataset. The losses of the training process and the confusion matrix are presented in Fig. 8b and 9b, respectively.

The complete ANN-based handover scheme is obtained by combining the two well-trained ANNs. The proposed ANN-based approach will be compared with the other three benchmarks in terms of user throughput, handover rate, and robustness in the following sections.

C. HANDOVER ACCURACY

1000 sets of labeled data are randomly chosen from the test set to evaluate the handover accuracy of the four handover methods. The accuracy performance is presented in Fig. 10. It shows that the proposed ANN-based handover scheme is able to achieve the highest handover accuracy of 95.1% with F_1 score equivalent to 0.89. In addition, the handover accuracy of K-LR and K-SVM methods are similar, which agrees with the conclusion of our previous study in [17]. They can also achieve handover accuracy of above 90%; however, their F_1 scores, which equal 0.79 and 0.81 respectively, are lower than that of the proposed ANN-based method. The numerical results of these two methods are slightly different from those in [17] since different test sets are used in these two studies. The ANN* benchmark has the lowest handover accuracy of 83.1% and the worst F_1 score of 0.64.

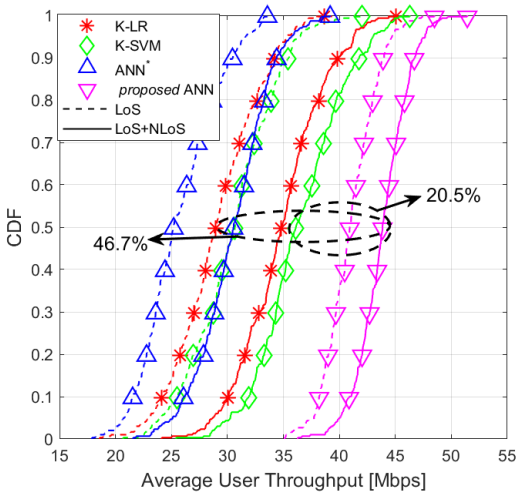

FIGURE 11. The CDF plot of average user throughput of the proposed ANN-based handover scheme and benchmarks.

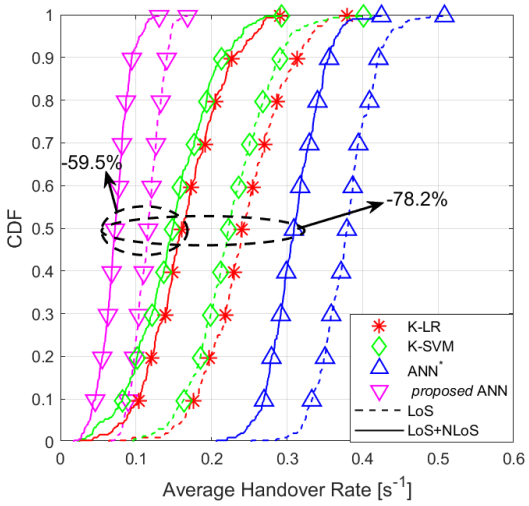

FIGURE 12. The CDF plot of handover rate of the proposed ANN-based handover scheme and benchmarks.

D. USER THROUGHPUT

Fig. 11 shows the cumulative distribution function (CDF) plot of average user throughput under two different situations: i) only LoS component is considered, and ii) both LoS and NLoS components are taken into account. It is found that for all four methods, the user throughput that considers both LoS and NLoS components is always greater than that which considers the LoS component only. This is because the NLoS component can significantly increase the received signal strength of UE, especially for those UE close to the wall, where LoS signal is often extremely low but the NLoS part is strong. Additionally, the proposed ANN-based scheme can always achieve the highest user throughput, which is around $20.5 - 46.7\%$ higher than that of the benchmarks. Furthermore, it shows that the CDF curves of the proposed scheme are the sloppiest, which indicates that our method has the best robustness performance as compared to the benchmarks. The reason is that our approach takes into account multiple attributes to make the handover decision.

E. HANDOVER RATE

The handover performance of four different handover algorithms is presented in Fig. 12. Same as Section IV-C, it can be concluded that, for all four methods, the handover performance with both LoS and NLoS components considered is always better than that with LoS component only, which indicates that NLoS component can largely improve the optical channel quality. The average handover rates of the proposed ANN-based scheme are the lowest, whereas those of the ANN* are the highest. The performance of the K-LR is similar to that of the K-SVM, which agrees with what we found in [17]. Specifically, the proposed ANN-based algorithm can reduce the handover rates by around 59.5% and 78.2% as compared to K-SVM and ANN* algorithms.

F. ROBUSTNESS

A good handover algorithm should not only boost the transmission rate and avoid unnecessary handovers but also adapt

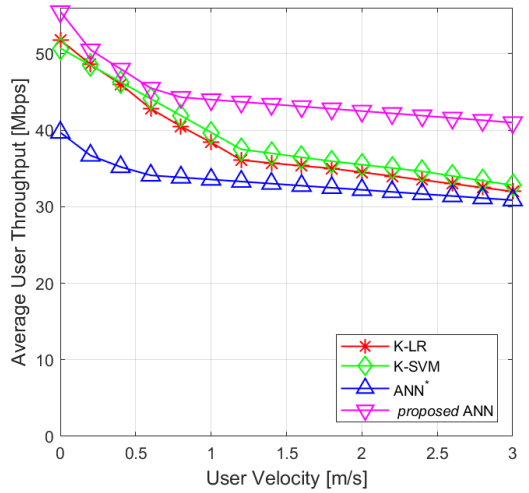

FIGURE 13. Average user throughput versus user velocity.

to different working scenarios. In other words, it is supposed to show robustness against different working scenarios. We first examine the effect of user velocity on the performance of different algorithms. Fig. 13 shows the average user throughput as a function of user velocity. It shows that the data rates provided by all four methods decrease as the user velocity increases; however, the proposed ANN-based approach and another ANN-based method (ANN*) have relatively smaller variations, since the user velocity has been attributed to the network selection in these two methods. Our proposed algorithm provides the highest user throughput at different velocities; in the meanwhile, it is more immune to speed variations than K-SVM and K-LR benchmarks. The influence of the user velocity on the handover rate is presented in Fig. 14. The handover rates increase as the velocity increases for all four methods, among which ANN* has the greatest handover rate, and our proposed algorithm has the lowest handover rate and the best robustness performance. The proposed ANN-based method can avoid around 60% and

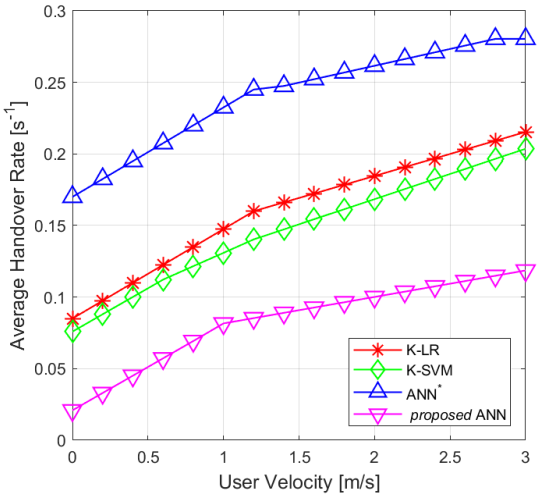

FIGURE 14. Average handover rate versus user velocity.

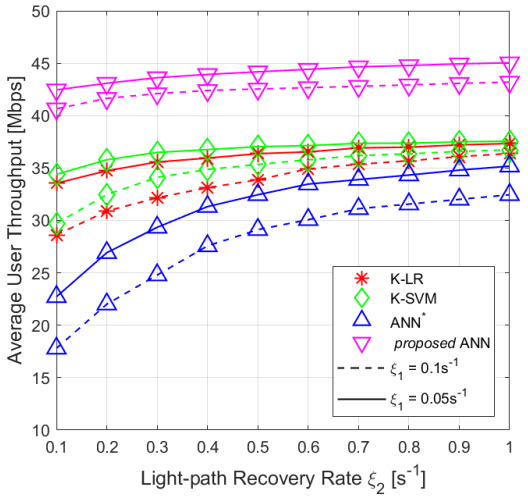

FIGURE 15. Average user throughput versus channel quality.

75% handoffs as compared to the K-SVM and the ANN* algorithms, which agrees with our observation from Fig. 12.

Fig. 15 and Fig. 16 compare the average user throughput and the handover rate performance of the proposed scheme and the benchmarks under different channel conditions. As we know, the quality of the optical channel is determined by interruption and recovery rates together. The interruption rate ξ_1 is chosen as 0.05s^{-1} and 0.1s^{-1}, whilst the recovery rate ξ_2 ranges from 0.1s^{-1} to 1s^{-1}. The increase in ξ_1 means that the light path is interrupted more frequently; in other words, the channel quality becomes "worse". In contrast, the increase in ξ_2 indicates that a blocked optical channel has a greater chance of recovery. In Fig. 15, it is found that the average user throughput of all four methods increases as ξ_1 decreases or as ξ_2 increases, which agrees with our expectation. Additionally, the average data rate provided by the ANN-based algorithm is always the highest; in the meanwhile, its variation is the smallest which indicates that our method has the best robustness performance. Fig. 16 shows the average handover rates of the

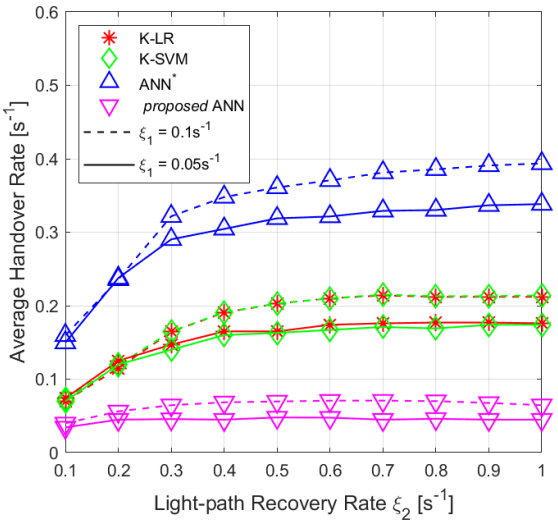

FIGURE 16. Average handover rate versus channel quality.

proposed ANN-based method as compared with the benchmarks. It shows that ANN*, K-SVM, and K-LR methods have much higher handover rates and they are more susceptible to network condition variations. Our ANN-based algorithm, in contrast, can significantly reduce the handover rates under different channel qualities, and at the same time, maintain the strongest robustness.

V. CONCLUSION

In this paper, the handover problem in the HLWNet is regarded as a binary classification problem and an ANN-based handover scheme is proposed as a solution. The proposed handover scheme consists of two ANNs, of which one is for making the handover decision from LiFi to WiFi and the other one is for the handover decision from WiFi to LiFi. To obtain reliable and realistic simulation results, we build a comprehensive simulation model that includes channel quality, user movement, light-path blockage, and device orientation. In addition, a novel approach is introduced to generate labeled datasets for supervised training. After being trained with the pre-labeled datasets, the ANN models are able to achieve above 95% handover accuracy. The proposed ANN-based handover scheme is then evaluated and compared with another ANN-based method and two handover schemes using pattern recognition techniques. The simulation results show that, compared with benchmarks, the proposed method can significantly increase user throughput by around $20.5-46.7\%$ and reduce handover rates by around $59.5-78.2\%$. Furthermore, the proposed method also shows great robustness against different working scenarios. Our work is novel and it shows that the neural network can be a potentially robust solution to the handover problem in heterogeneous networks. We believe that this work can play an important role in future research on the next-generation wireless network which is expected to be composed of ultra-dense networks with LoS communication links such as LiFi and millimeter wave networks.

REFERENCES

[1] X. You et al., "Towards 6G wireless communication networks: Vision, enabling technologies, and new paradigm shifts," *Sci. China Inf. Sci.*, vol. 64, no. 1, pp. 1–74, 2021.
[2] I. Lee and K. Lee, "The Internet of Things (IoT): Applications, investments, and challenges for enterprises," *Bus. Horizons*, vol. 58, no. 4, pp. 431–440, 2015.
[3] S. Dang, O. Amin, B. Shihada, and M.-S. Alouini, "What should 6G be?" *Nature Electron.*, vol. 3, no. 1, pp. 20–29, Jan. 2020.
[4] H. Haas, L. Yin, Y. Wang, and C. Chen, "What is LiFi?" *J. Lightw. Technol.*, vol. 34, no. 6, pp. 1533–1544, Mar. 15, 2016.
[5] M. S. Islim, R. X. Ferreira, X. He, E. Xie, S. Videv, S. Viola, S. Watson, N. Bamiedakis, R. V. Penty, I. H. White, A. E. Kelly, E. Gu, H. Haas, and M. D. Dawson, "Towards 10 Gb/s orthogonal frequency division multiplexing-based visible light communication using a GaN violet micro-LED," *Photon. Res.*, vol. 5, no. 2, pp. A35–A43, 2017.
[6] M. A. Arfaoui, M. D. Soltani, I. Tavakkolnia, A. Ghrayeb, C. M. Assi, M. Safari, and H. Haas, "Invoking deep learning for joint estimation of indoor LiFi user position and orientation," *IEEE J. Sel. Areas Commun.*, vol. 39, no. 9, pp. 2890–2905, Sep. 2021.
[7] X. Wu, M. D. Soltani, L. Zhou, M. Safari, and H. Haas, "Hybrid LiFi and WiFi networks: A survey," *IEEE Commun. Surveys Tuts.*, vol. 23, no. 2, pp. 1398–1420, 2nd Quart., 2021.
[8] X. Wu and D. C. O'Brien, "A novel machine learning-based handover scheme for hybrid LiFi and WiFi networks," in *Proc. IEEE Globecom Workshops (GC Wkshps*, Dec. 2020, pp. 1–5.
[9] G. Ma, R. Parthiban, and N. Karmakar, "An adaptive handover scheme for hybrid LiFi and WiFi networks," *IEEE Access*, vol. 10, pp. 18955–18965, 2022.
[10] J. Hou and D. C. O'brien, "Vertical handover-decision-making algorithm using fuzzy logic for the integrated radio-and-OW system," *IEEE Trans. Wireless Commun.*, vol. 5, no. 1, pp. 176–185, Jan. 2006.
[11] Y. Wang, X. Wu, and H. Haas, "Fuzzy logic based dynamic handover scheme for indoor Li-Fi and RF hybrid network," in *Proc. IEEE Int. Conf. Commun. (ICC)*, May 2016, pp. 1–6.
[12] F. Wang, Z. Wang, C. Qian, L. Dai, and Z. Yang, "Efficient vertical handover scheme for heterogeneous VLC-RF systems," *J. Opt. Commun. Netw.*, vol. 7, no. 12, pp. 1172–1180, 2015.
[13] E. Stevens-Navarro, V. W. S. Wong, and Y. Lin, "A vertical handoff decision algorithm for heterogeneous wireless networks," in *Proc. IEEE Wireless Commun. Netw. Conf.*, Mar. 2007, pp. 3199–3204.
[14] X. Bao, W. Adjardjah, A. A. Okine, W. Zhang, and J. Dai, "A QoE-maximization-based vertical handover scheme for VLC heterogeneous networks," *EURASIP J. Wireless Commun. Netw.*, vol. 2018, no. 1, pp. 1–12, Dec. 2018.
[15] D. Niyato and E. Hossain, "Dynamics of network selection in heterogeneous wireless networks: An evolutionary game approach," *IEEE Trans. Veh. Technol.*, vol. 58, no. 4, pp. 2008–2017, May 2009.
[16] S. Liang, Y. Zhang, B. Fan, and H. Tian, "Multi-attribute vertical handover decision-making algorithm in a hybrid VLC-Femto system," *IEEE Commun. Lett.*, vol. 21, no. 7, pp. 1521–1524, Jul. 2017.
[17] G. Ma, R. Parthiban, and N. Karmakar, "Novel handover algorithms using pattern recognition for hybrid LiFi networks," in *Proc. IEEE Symp. Comput. Commun. (ISCC)*, Jun. 2022, pp. 1–7.
[18] T. Wang, C.-K. Wen, H. Wang, F. Gao, T. Jiang, and S. Jin, "Deep learning for wireless physical layer: Opportunities and challenges," *China Commun.*, vol. 14, no. 11, pp. 92–111, Oct. 2017.
[19] Y. Sun, M. Peng, Y. Zhou, Y. Huang, and S. Mao, "Application of machine learning in wireless networks: Key techniques and open issues," *IEEE Commun. Surveys Tuts.*, vol. 21, no. 4, pp. 3072–3108, 4th Quart., 2019.
[20] H. Ye, G. Y. Li, and B.-H. F. Juang, "Deep reinforcement learning based resource allocation for V2V communications," *IEEE Trans. Veh. Technol.*, vol. 68, no. 4, pp. 3163–3173, Apr. 2019.
[21] H. Alshaer and H. Haas, "SDN-enabled Li-Fi/Wi-Fi wireless medium access technologies integration framework," in *Proc. IEEE Conf. Standards Commun. Netw. (CSCN)*, Oct. 2016, pp. 1–6.
[22] G. Cossu, R. Corsini, and E. Ciaramella, "High-speed bi-directional optical wireless system in non-directed line-of-sight configuration," *J. Lightw. Technol.*, vol. 32, no. 10, pp. 2035–2040, May 15, 2014.
[23] X. Wu, D. C. O'Brien, X. Deng, and J.-P.-M. G. Linnartz, "Smart handover for hybrid LiFi and WiFi networks," *IEEE Trans. Wireless Commun.*, vol. 19, no. 12, pp. 8211–8219, Dec. 2020.
[24] S. Shao, G. Liu, A. Khreishah, M. Ayyash, H. Elgala, T. D. Little, and M. Rahaim, "Optimizing handover parameters by Q-learning for heterogeneous radio-optical networks," *IEEE Photon. J.*, vol. 12, no. 1, pp. 1–15, Feb. 2020.
[25] L. Yin, X. Wu, and H. Haas, "Indoor visible light positioning with angle diversity transmitter," in *Proc. IEEE 82nd Veh. Technol. Conf. (VTC-Fall)*, Sep. 2015, pp. 1–5.
[26] G. Cybenko, "Approximation by superpositions of a sigmoidal function," *Math. Control, Signals Syst.*, vol. 2, no. 4, pp. 303–314, 1989.
[27] N. M. Alotaibi and S. S. Alwakeel, "A neural network based handover management strategy for heterogeneous networks," in *Proc. IEEE 14th Int. Conf. Mach. Learn. Appl. (ICMLA)*, Dec. 2015, pp. 1210–1214.
[28] X. Tan, G. Chen, and H. Sun, "Vertical handover algorithm based on multi-attribute and neural network in heterogeneous integrated network," *EURASIP J. Wireless Commun. Netw.*, vol. 2020, no. 1, pp. 1–21, Dec. 2020.
[29] S. Ruder, "An overview of gradient descent optimization algorithms," 2016, *arXiv:1609.04747*.
[30] I. Goodfellow, Y. Bengio, and A. Courville, *Deep Learning*. Cambridge, MA, USA: MIT Press, 2016, [Online]. Available: http://www.deeplearningbook.org
[31] T. Fawcett, "An introduction to ROC analysis," *Pattern Recognit. Lett.*, vol. 27, no. 8, pp. 861–874, Jun. 2006.

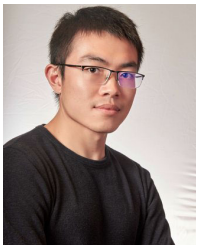

GUANGHUI MA (Member, IEEE) received the bachelor's degree in electrical engineering from Xi'an Jiaotong University, China, in 2016, and the master's degree (Hons.) in engineering from the University of Melbourne, in 2018. He is currently pursuing the Ph.D. degree with Monash University, Australia.

His research interests include visible light communication, and heterogeneous optical and RF networks.

RAJENDRAN PARTHIBAN (Senior Member, IEEE) received the B.E. degree (Hons.) and the Ph.D. degree in optical networks from the University of Melbourne, Australia, in 1997 and 2004, respectively.

He joined as a Lecturer with the School of Engineering, Monash University Malaysia, in 2006, where he was a Professor, in 2022, and he has been the Deputy Head of School (Education), since August 2010. He moved to the Faculty of Engineering, Monash University, Australia, as the Associate Dean (Education), and has been a Professor, since August 2022. He has over 90 journals and conference publications. His research interests include optical networks, visible light communications, vehicular communication, the Internet of Things, and engineering education. He obtained external grants worth over A$800k. Under his supervision, 15 Ph.D. and two master's students have completed their studies.

Dr. Parthiban is a Senior Member of Optica [formerly known as the Optical Society of America (OSA)].

NEMAI KARMAKAR (Senior Member, IEEE) received the master's degree in electrical engineering from the University of Saskatchewan, Canada, in 1991, and the Ph.D. degree from the University of Queensland, Australia, in 1999.

He has over 20 years of teaching, design, and development experience in antennas, microwave active and passive circuits, and RFIDs in Canada, Australia, and Singapore. He is currently an Associate Professor with the Department of Electrical and Computer Systems Engineering, Monash University, Australia. He has authored or coauthored over 400 refereed journals and conference papers, 24 book chapters, and eight books. His research interests include RFID, smart antennas for mobile and satellite communications, the Internet of Things (IoT), and visible light communication.